# Scroll compressor modelling for heat pumps using hydrocarbons as refrigerants

Paul Byrne, Redouane Ghoubali, Jacques Miriel

## ▶ To cite this version:

## HAL Id: hal-00926697

## https://hal.archives-ouvertes.fr/hal-00926697

Submitted on 10 Jan 2014

# Scroll compressor modelling for heat pumps using hydrocarbons as refrigerants

Paul **BYRNE\***, Redouane **GHOUBALI**, Jacques **MIRIEL**

Université Européenne de Bretagne

Université de Rennes1, Laboratoire LGCGM, Equipe MTRhéo

IUT Génie Civil, 3 rue du Clos Courtel, BP 90422, 35704 Rennes Cedex 7, France

Phone: +33 2 23 23 42 97 - Fax: +33 2 23 23 40 51

\* corresponding author: paul.byrne@univ-rennes1.fr

## ABSTRACT

Hydrocarbons are today considered as promising alternatives to hydrofluorocarbons thanks to their low environmental impact and their easy implementation. However, some precautions have to be taken to thwart their flammability. European regulations impose to take stringent measures regarding components and to install heat pumps in unoccupied spaces. Nevertheless manufacturers keep working on components for hydrocarbons. In the frame of a research project on heat pumps for simultaneous heating and cooling, an R407C prototype working with a scroll compressor was built and tested. A near-industrial prototype is today being designed for propane with the help of recent modelling techniques. After having detailed the main issues regarding hydrocarbons as refrigerants, this article reviews scroll compressor modelling studies and presents the development of a thermodynamically realistic scroll compressor model. It was first developed for R407C and then adapted to thermodynamic properties of hydrocarbons and to other sizes of compressors.

*Keywords: compressor, scroll, model, hydrocarbons*

# NOMENCLATURE

**Letter symbols:**

A          heat exchange surface area ($m^2$)

D          hydraulic diameter (m)

e          edge length of a cube (m)

h          enthalpy ($J\ kg^{-1}$)

HP         high pressure (Pa)

LP         low pressure (Pa)

$\dot{m}$          mass flow rate ($kg\ s^{-1}$)

n          polytropic exponent (-)

Nu         Nusselt number (-)

P          pressure (Pa)

Pr         Prandtl number (-)

$\dot{Q}$          thermal capacity (W)

Re         Reynolds number (-)

T          temperature (K)

U          heat transfer coefficient ($W\ m^{-2}\ K^{-1}$)

u          velocity ($m\ s^{-1}$)

$V_s$          swept volume ($m^3\ s^{-1}$)

$\dot{W}$          compression work (W)

**Greek symbols:**

$\gamma$          isentropic exponent (-)

$\lambda$          thermal conductivity ($W\ m^{-1}\ K^{-1}$)

$\nu$          viscosity ($m^2\ s^{-1}$)

**Superscripts:**

n          polytropic exponent (-)

$\gamma$          isentropic exponent (-)

m          parameter for Dittus-Boelter correlation

**Subscripts:**

| | |
|---|---|
| 0 | original value |
| amb | ambient |
| cd | condensation |
| ev | evaporation |
| ex | exhaust |
| HC | hydrocarbon |
| in | internal |
| nom | nominal |
| su | suction |
| w | wall |

**abreviations:**

| | |
|---|---|
| ATEX | explosive atmospheres |
| COP | coefficient of performance (-) |
| DHW | domestic hot water |
| GWP | global warming potential ($kg_{CO2}$) |
| HC | hydrocarbon |
| HFC | hydrofluorocarbon |
| HFO | hydrofluoroolefin |
| HPS | heat pump for simultaneous heating and cooling |
| LMTD | logarithmic mean temperature difference (K) |
| TEWI | total equivalent warming impact ($kg_{CO2}$) |

# 1. INTRODUCTION

The study presented in this article is a part of a project on heat pumps for simultaneous heating and cooling (HPS), in which our research team worked on the implementation of R407C and natural refrigerant $CO_2$ (Byrne et al., 2009). At that stage of the project, we were not able to build a near-industrial $CO_2$ HPS because components were not easily available for the high operating pressures involved in the transcritical cycle of carbon dioxide. A first R407C prototype providing 15 kW heating capacity was then built, tested and simulated (Byrne et al., 2011a, 2011b, 2012). It can produce hot and cold water in two different water tanks at the same time (simultaneous mode), only hot water (heating mode) or only cold water (cooling mode). The main characteristic of the HPS is to operate using an alternation of two modes during winter. In a heating mode, the HPS produces heat and also stores some energy recovered by subcooling of the refrigerant in the cold water tank (not or rarely used for cooling during winter). The water tank temperature rises up to a set point and the simultaneous mode is launched. During the simultaneous mode operation, the heat pump performance is increased thanks to a higher evaporating temperature using temperature-controlled water than using ambient air as a heat source. The objective of developing a second prototype with a near-industrial design using a fluid with low environmental impact is still the main goal of the project. HFOs being protected by patents were taken out of the list of the possible environmentally friendly refrigerants. The corrosive effect of ammonia in presence of copper would have led us to buy more expensive components made of stainless steel. Our heat pump would also have been submitted to more restrictive regulations. Finally, $CO_2$ technology staying difficult to acquire easily and to handle, we chose to use propane for the new prototype as this fluid is the most commonly used hydrocarbon for the applications of the HPS. The refrigerant charge of this prototype is less than 5 kg, which is the charge limit for category A (general occupancy) and indirect systems according to European regulation EN 378 (2008), corresponding to systems in which all the refrigerant containing parts are located in an unoccupied machinery room or in open air of unoccupied spaces. The issues regarding the implementation of a scroll compressor instead of a reciprocating compressor to this new HPS prototype working with a hydrocarbon are discussed in this study. Scroll compressors are well adapted to the applications targeted in our project and show higher efficiencies, low torque variations, low noise, reliability and tolerance to refrigerant droplets (Winandy, 2002a).

The objectives of this article are first to give the characteristics of hydrocarbons that are important for the application of low to medium capacity heat pumps, then to review the modelling techniques available in the literature to assess the performance of scroll compressors and finally, to present the development of a simplified scroll compressor model for future performance evaluation of a heat pump for simultaneous heating and cooling working with propane. The model was first developed for a R407C scroll compressor and validated using experimental results. Then the model was adapted to refrigerants R290 (propane), R600a (isobutane) and R1270 (propylene or also called propene). A simulation comparison is carried out to evaluate the mass flow rate and input power discrepancies and discharge temperature differences between R407C and hydrocarbons. Finally an adaptation procedure was applied to the model to deal with a change of the compressor size. The simulation results are compared to experimental data obtained on a homemade prototype or another set of data provided by a compressor manufacturer.

## 2. HYDROCARBONS AS REFRIGERANTS

Since decades hydrocarbons have been used in some applications such as domestic refrigeration and small capacity exhaust air heat pumps (Granryd, 2001) but they have not yet entered some markets on which their thermodynamic and environmental properties would have let them become alternatives to R22. This paragraph presents the main characteristics of hydrocarbons that explain this situation such as safety and standards, environmental impact and thermodynamic properties.

### 2.1. Safety and European standards

Hydrocarbons are highly flammable fluids. Palm (2008) presents the flammability properties of isobutane (R600a), propane (R290) and propene or propylene (R1270) and argues that because of high flammability compressors are either small or large. Small compressors contain a low charge of refrigerant. Large compressors are used in the industry sector in which safety measures are less restrictive because of imposed monitoring and regular maintenance. No medium-sized compressors existed for heat pumps in residential or tertiary applications. Palm (2008) also reviews the compressor types available in the market. Only rotary, reciprocating and centrifugal compressors were available.

Precautions have to be taken to minimize contact between the refrigerant and components likely to generate sparks such as rotating elements of the compressor or solenoid valves. Scroll compressors present extended

contact surfaces or longer contact lines between the orbiting scroll and the fixed scroll than between moving and static parts of other types of compressors. The surface roughness of moving parts can today be minimized and controlled by evolved manufacturing processes (Jiang et al., 2003). The ignition of the hydrocarbon refrigerant can also happen through a defect of the winding insulation inside the compressor. As for solenoid valves, ATEX certification (Explosive Atmospheres) is required to commercialize hydrocarbon compressors (European Standard EN 60079-10-1, 2009). This document imposes dispositions to take to avoid substance leakage and spark creation. Following European Regulation EN 378 (2008), the charge is limited to 5 kg of hydrocarbon in a refrigeration machine placed in an unoccupied space opened to public access (indirect systems). The charge limit is 1.5 kg if part of the refrigerant circuit is in an occupied space (direct systems).

Since the review study of Palm, Adamson (2008) presented ATEX-certified scroll compressors for hazardous areas and the maintainable effect of hydrocarbons on the refrigeration equipment during a four-year period of operation. Arnemann et al. (2012) carried out experiments on scroll compressors with hydrocarbons. Scroll compressors originally for R407C and R404A were tested with propane and propylene. The experiments do not report problems concerning flammability of hydrocarbons. However, the flammability issue still limits the widespread of the technology in all sectors.

### 2.2. Performance of thermodynamic cycles

A previous publication (Byrne, 2013) presents the thermodynamic performance of some refrigerants in heat pump cycles for space heating and domestic hot water heating (DHW). Table 1 reports the values of the previous publication for the fluids considered in the following simulation study and adds more values for a cooling mode. The heating COPs for space heating and DHW production and the cooling COP are presented. The simulations were run using the cycle analysis tool of Coolpack (Technical University of Denmark, 1998) working under the Engineering Equation Solver environment (Klein and Alvarado, 1992).

The following assumptions were taken into account for all fluids:

- Superheat and subcooling equal to 0 K.
- No pressure losses in the heat exchangers.

- No suction gas heat exchanger.

- Isentropic efficiency equal to 0.7.

- No heat loss at the compressor.

- No "unuseful superheat" in the suction line.

- Air temperature variation through heat exchangers is 8 K.

- Water temperature variation through heat exchangers is 5 K.

- Temperature pinches in heat exchangers are equal to 5 K.

- Ambient air temperature is 7 °C in heating modes.

- Ambient air temperature is 30 °C in the cooling mode.

- Water heating temperature is 35 °C in the space heating mode.

- Water heating temperature is 65 °C in the domestic hot water production mode.

- Water cooling temperature is 7 °C in the cooling mode.

- The heat exchangers are assumed to be counter-flow.

Isentropic efficiency is kept constant and no heat loss at the compressor is modelled. These assumptions result in an unrealistic constant global efficiency of the compressor in spite of varied operating conditions. However, fixing initially these parameters enables to provide a clear view of the performance comparison of refrigerants in systems for distinguished applications. Source temperatures follow European standard EN14511 (2004) for heat pump testing. An ambient air temperature equal to 7 °C results in an evaporating temperature of -6 °C for an assumed air cooling of 8 K, except for the zeotropic mixture R407C, for which the temperature glide enables to reach an evaporating temperature of -1 °C at dew point. The chosen hot water production temperature implies higher condensing temperatures. It is assumed that temperature pinches in the heat exchangers are equal to 5 K. In the cooling mode, the cold water is produced at 7 °C. The resulting evaporating temperature is 2 °C for hydrocarbons and 7 °C (dew point) for R407C. The condensing temperatures are 40 °C, 70 °C and 43 °C respectively for space heating, DHW production and cooling modes.

Table 1 shows the simulation results in terms of coefficients of performance for space heating, DHW production and space cooling. R407C takes advantage of the 5 K-higher evaporating temperature in space

heating and cooling but does not outperform hydrocarbons in DHW production. Hydrocarbons show

equivalent performance because cycles have more or less the same properties. Isobutane R600a benefits

from a higher critical temperature than the other fluids especially regarding DHW COP and cooling COP.

The compressor performance depends on the fluid. However it was assumed constant in this first

comparison. Therefore table 1 will serve as a base of discussion in the section dedicated to the comparison

of compressor performance depending on the fluid.

**Table 1:** Heating COP in space heating, DHW COP and cooling COP of thermodynamic cycles working

with refrigerants R407C, R290, R600a and R1270.

| Fluid | Heating COP | DHW COP | Cooling COP |
|:---:|:---:|:---:|:---:|
| R407C | 4.60 | 2.39 | 4.26 |
| R290 | 4.12 | 2.34 | 3.66 |
| R600a | 4.19 | 2.45 | 3.77 |
| R1270 | 4.12 | 2.33 | 3.65 |

## 2.3. Environmental impact

Hydrocarbons are positioned as natural alternative refrigerants to halogenated substances. The ozone

depletion potential is zero. Their environmental impact is also very low in terms of global warming. The

GWP (global warming potential) of most common hydrocarbons such as propane (R290) is equal to 3 over a

100-year horizon. The TEWI (total equivalent warming impact) of a hydrocarbon heat pump system should

be low because of the higher performance of the thermodynamic cycle compared to most synthetic fluids;

the indirect part of the TEWI should be lower since it is calculated using the energy input to the compressor

and the direct part of the TEWI will be low due to the low GWP of hydrocarbons (Halimic et al., 2003).

Energetic performance of hydrocarbons is comparable to that of the fluorinated fluids in the same range of

pressures. The environmental impact is low compared to other refrigerants. These fluids are already widely

used in household applications like domestic refrigerators (Palm, 2008) since components have the same

technical characteristics as the ones for HFCs. Therefore hydrocarbons may also be envisaged as drop-in

substitutes to HFCs in heat pumps using the same technology as long as the European Regulations are

respected in terms of refrigerant charge limit and ATEX certification of equipment.

## 3. SCROLL COMPRESSOR MODELLING TECHNIQUES

Several studies were already carried out on more or less detailed compressor modelling. We distinguish three categories: geometrical models, semi-empirical models and empirical models. Table 2 summarizes the following scroll compressor models found in the literature. According to this review, the modelling technique which was estimated as the most appropriate is applied to an R407C scroll compressor.

### 3.1. Geometrical models

Chen et al. (2002a and 2002b) worked on a geometrical modelling of scroll compressors. A geometry study was conducted on the suction, compression and discharge chambers of the compressor. It combines the models of refrigerant flows in the suction and discharge processes, radial and flank leakage and heat transfers between the refrigerant and the scroll wraps. Blunier et al. (2009) developed a similar geometry description of the scroll compressor model. Tseng and Chang (2006) and Sun et al. (2010) also propose a design optimization of the scroll compressor using geometrical models. Rong and Wen (2009) used a simplified geometrical model to analyze tangential and axial leakage and related factors and their impact on performance. A lumped geometrical model of a scroll compressor with refrigeration injection is used to predict thermodynamic performance and compression process is presented by Wang et al. (2008). Qiang et al. (2013a and 2013b) present a dynamic model of scroll compressors to calculate pressure distribution, forces and moments on the scrolls surfaces and shaft and for different types of scroll wraps. Ooi & Zhu (2004) developed a scroll compressor model based on k-ε turbulence model to study the fluid flow and heat transfer in the compression chamber. Liu et al. (2009 and 2010) modeled very specific parts of scroll compressors: the bypass behaviors used in scroll compressor to prevent over-compression and frictional losses in bearings. These studies present very useful methods and results for design optimization of specific parts of compressors as injection or bypass port diameter, dimensions (orbiting radius, involute start and end angles…) or leakage reduction.

### 3.2. Semi-empirical models

Some geometrical models also use empirical equations. Park et al. (2002) present a general model of variable speed scroll compressor with refrigerant injection based on geometric data and injection conditions.

The model was verified by experimental data for no injection condition with satisfactory accuracy. The motor and mechanical efficiency calculated by test data in this paper were used by Wang et al. (2005) in geometrical model based on discretional initial angles of scroll involutes.

Cuevas and Lebrun (2009), Cuevas et al. (2010), Winandy et al. (2002a), Winandy and Lebrun (2002b) worked on a simplified scroll compressor model based on the main processes affecting the refrigerant during compression. It uses a fictitious wall to model heat exchanges within the compressor and between the compressor and the ambiance. It is able to compute the following variables: mass flow rate, power input, discharge temperature, thermal capacities at suction heating-up and discharge cooling-down and ambient losses. Duprez et al. presented two papers (2007 and 2010) on a modelling technique for reciprocating and scroll compressors based on the first model presented by Winandy et al. (2002a). Some adaptations were made to this thermodynamically realistic semi-empirical technique. Accurate results are also obtained, having average deviations less than 3% on mass flow rates and power consumptions for scroll compressors. Cuevas et al. (2012) investigated the characteristics of an automotive electric scroll compressor using the same base model. Madani et al. (2011) used another model that emphasize on the built-in volume ratio, which corresponds to the volume of the gas pocket immediately after closing the suction port over the volume just before opening the discharge port. It is fixed by the geometry of the compressor and defines an isentropic process part of the real compression (Winandy et al., 2002a). Kim et al. (2008) worked on a $CO_2$ heat pump water heater cycle with expander-compressor unit. A thermodynamic model with fixed volumetric and isentropic efficiencies is presented. Li (2013) proposes a simplified steady-state modelling for variable speed reciprocating, scroll and piston rotary compressors. The compression is modelled as polytropic such as in the article of Guo et al. (2011). Many parameters are used to calibrate the model. Choi et al. (2011) models a scroll compressor using a lumped parametric model. Lee et al. (2013) compared different approaches of modelling: constant-polytropic-coefficient, constant-polytropic-efficiency and Mallen-Saville approaches. The first approach is the simplest but leads to higher errors than the other two approaches.

Following this part of the literature review, it appears that semi-empirical models are used to assess the performance of a heat pump or a refrigerating machine under various operating conditions. The modelling

structure is validated with real compressor data. The output variables of the models are generally mass flow rate, power and discharge temperature.

## 3.3. Empirical models

This type of macro models is usually used as submodels in simulation of global thermodynamic systems. Techarungpaisan et al. (2007) present an empirical model of compressor used in the simulation of a split type air-conditioner. The efficiencies of the compressor are fixed and the main outputs of the model are based on the manufacturers' data curves. Kinab et al. (2010) proposed a global heat pump model for seasonal performance optimization. It also uses an empirical model for the compressor efficiencies and leads to results in pretty good agreement with those of a test bench. A previous study carried out in our laboratory deals with the simulation of a heat pump for simultaneous heating and cooling (HPS) using HFC or $CO_2$ as a working fluid (Byrne et al., 2009). Isentropic efficiency was given by empirical formulas. Another larger study used empirical compressor efficiency (Byrne et al., 2012). Good agreement was obtained for the mass flow rate ($\pm 7\%$) and the electric power ($\pm 5\%$). However this model was only valid for the studied HPS prototype.

## 3.4. Summary on scroll compressor model review

Table 2 classifies the models by giving the model type (geometrical, semi-empirical and empirical) and an uncorrelated level of accuracy. The variables needed to simulate a refrigeration system for seasonal performance evaluation are the input power consumption, the discharge temperature and the mass flow rate. The last two variables are used in the other components of the system: condenser(s), evaporator(s) and expansion device to simulate the complete heat pump system. They can be obtained with sufficient accuracy using a semi-empirical model with constant polytropic coefficient. The interesting aspect of such type of model is that the same method could be adapted to other fluids and to other compressor sizes. Some of the models (Li (2012 and 2013), Duprez et al. (2007), Dupez et al. (2010)) use parameters that do not represent any physical value. Table 2 shows that many scroll compressor models neglect the impact of lubricant in the compression process while giving results with high accuracy. Indeed neglecting oil behaviour seems reasonable because with a variation of oil sump temperature, the solubility of refrigerant in oil and the

heating-up of refrigerant vary with compensatory effects. Navarro et al. (2012) propose a theoretical analysis and correlations to calculate oil sump temperature in hermetic compressors (scroll and reciprocating). The tested scroll compressor showed an oil sump temperature 10 K lower than for reciprocating compressors. This result indicates that the suction heating-up of refrigerant before entering the scrolls will be less influenced by the oil temperature and also participates to the choice of neglecting oil behaviour in scroll compressor modelling.

**Table 2:** Summary of publications on scroll compressor models

| Model type | Authors | Main outputs | Accuracy | Oil effects |
|---|---|---|---|---|
| Geometrical | Blunier et al.(2009) | Mass flow rate, pressure in compression chambers | For speeds higher than 2500 rpm, the model fails to predict an accurate mass flow. | Neglected |
| Geometrical | Chen et al. (2002a, 2002b) | Mass flow rate, compressor power and discharge temperature | Calculated data is very close to the measured data (error of 3 %) | Taken into account |
| Geometrical | Liu et al. (2009) | Volumetric efficiency, isentropic efficiency , mass flow rate | Mass flow -3.2 % to 0.8 %, $\eta_V$ -2.7 % to +1.2 %, $\eta_C$ -0.7% to +2% | Neglected |
| Geometrical | Liu et al. (2010) | Compressor efficiency, volumetric efficiency | Compressor efficiency 3.3% volumetric efficiency 3.5%. | Taken into account |
| Geometrical | Ooi and Zhu (2004) | Pressure, velocity, temperature, Convective heat transfer using CFD (k-ε turbulence model) | Properties in the chamber, except pressure, are highly spatially distributed. | Neglected |
| Geometrical | Qiang et al. (2013a, 2013b) | Pressure distribution, forces, moments and power | Depending on the scroll type. 6.1 % relative deviation at design speed for a single wrap air scroll compressor | Neglected |
| Geometrical | Rong and Wen (2009) | Leakage ratios, refrigerant mass in chambers, discharge pressure and temperature | Only numerical | Neglected |
| Geometrical | Sun et al. (2010) | Isentropic efficiency, volumetric efficiency | Only numerical | Neglected |
| Geometrical | Tseng and Chang (2006) | COP and cooling capacity | Cooling capacity 2.53 % and COP 1.69 % | Taken into account |
| Geometrical | Wang et al. (2008) | Mass flow rate, discharge temperature, compressor power | Mass flow rate varies from -3 % to +4 %. Shaft power is between -2 % and +3 %. Discharge temperature from -1 % to +1 %. | Neglected |
| Geometrical/ semi empirical | Park et al. (2002) | Mass flow rate, compressor power and discharge temperature | Error of 10% for 90% of experimental data | Neglected |
| Geometrical/ semi empirical | Wang et al. (2005) | Mass flow rate, compressor power, (Motor and mechanical efficiency provided by (Park, et al., 2002)) | Mass flow rate ±2.5 and motor power is between -2 and 5 % | Neglected |
| Semi-empirical | Choi et al. (2011) | Mass flow rate and discharge enthalpy | ±10 % on heating and cooling capacity | Neglected |
| Semi empirical | Cuevas et al. (2009, 2010) | Mass flow rate, exhaust temperature, compressor power | Exhaust temperature of ±1.0 K, Mass flow rate of ±2 g s-1 and compressor power of ±60 W. | Taken into account |
| Semi-empirical | Duprez et al. (2007, 2010) | Mass flow rate, compressor power and heat flow at the condenser | 3% on mass flow rate and less than 10% on input compressor power | Neglected |
| Semi-empirical | Guo et al. (2011) | Mass flow rate, compressor power and discharge enthalpy | Maximum deviation less than 10 % | Neglected |
| Semi-empirical | Kim et al. (2008) | COP, Isentropic efficiency, volumetric efficiency, mechanical efficiency | Only numerical | Neglected |
| Semi-empirical | Lee et al. (2013) | Isentropic efficiency, mass flow rate and compressor power | Less than 10 % error on isentropic efficiencies and power and less than 2 % error on mass flow rate | Neglected |
| Semi-empirical | Li (2012, 2013) | Mass flow rate, compressor power and discharge temperature | Around 5 % on mass flow rate and compressor power and less than 4 K on discharge temperature difference | Neglected |
| Semi-empirical | Madani et al. (2011) | Mass flow rate and compressor power | Less than 10 % error on compressor power | Neglected |
| Semi-empirical | Winandy (2002a, 2002b) | Mass flow rate, compressor power and discharge temperature | Less than 5 % on mass flow rate and compressor power and from -5 K to 5 K on discharge temperature | Neglected |
| Empirical | Byrne et al. (2009, 2012) | Mass flow rate and compressor power | ±7 % on mass flow rate and ±5 % on compressor power | Neglected |
| Empirical | Kinab et al. (2010) | Mass flow rate and compressor power | ±5 % on compressor power and less than ±2 % on mass flow rate | Neglected |
| Empirical | Techarung-paisan et al. (2007) | Mass flow rate, compressor power and discharge temperature | Little over-prediction, good tendency prediction | Neglected |

### 3.5. R407C scroll compressor model

This section describes the modelling procedure we used to develop a scroll compressor model and the validation steps by comparison with experimental data obtained with the scroll compressor of a R407C HPS. The modelling procedure is based on the model of Winandy et al. (2002a), in which the refrigerant state evolution is decomposed. It uses special assumptions, some of which are inspired by Duprez et al. (2007 and 2010). The difference with previous models relies on the compression process that is assumed to follow a polytropic evolution. The objective is here to use constant heat transfer values between the refrigerant and the crankcase at high and low pressure and between the crankcase and the ambiance as parameters for model calibration. The simulation software is EES (Klein and Alvarado, 2000). The model calculates the refrigerant mass flow rate, the input power and the discharge temperature using the suction temperature and high and low pressures as input variables and internal heat exchange coefficients as parameters.

### 3.5.1. General equations

Transformations applied to the refrigerant through the compressor can be defined following figure 1. Three steps are involved: suction heating up (from su to su1), polytropic compression (from su1 to ex1) and discharge cooling down (from ex1 to ex). $\dot{W}_{loss}$ corresponds to electromechanical losses and $\dot{W}_{in}$ to the internal compression power delivered to the refrigerant.
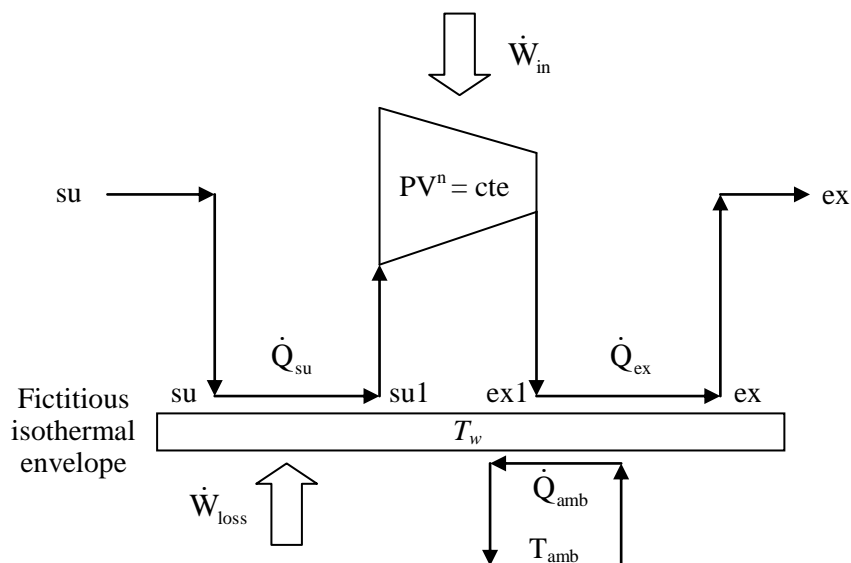


**Figure 1:** Refrigerant transformations through the compressor model

The refrigerant mass flow rate is given by equation 1 where $V_s$ in $m^3 \ s^{-1}$ is the constant swept volume provided by the manufacturer and $v_{su1}$ is the specific volume at the end of the suction heating-up process.

$$\dot{m} = \frac{V_s}{v_{su1}} \tag{1}$$

The fictitious wall is assumed in a steady state at a user-defined constant temperature, like in the publication of Duprez et al. (2007), at a mean value between temperatures at suction and exhaust points following equation 2.

$$T_w = \frac{T_{ex} + T_{su}}{2} \tag{2}$$

Heat transfers with the fictitious wall are supposed to be balanced and equation 3 can be stated.

$$\dot{W}_{loss} + \dot{Q}_{ex} - \dot{Q}_{su} - \dot{Q}_{amb} = 0 \tag{3}$$

Heat exchange at suction heating-up can be modelled using the LMTD method (Equation 4).

$$\dot{Q}_{su} = UA_{su} \cdot \left( \frac{T_{su1} \text{-} T_{su}}{ln \dfrac{T_w \text{-} T_{su}}{T_w \text{-} T_{su1}}} \right) \tag{4}$$

This thermal capacity is also defined by equation 5.

$$\dot{Q}_{su} = \dot{m} \cdot \left( h_{su1} - h_{su} \right) \tag{5}$$

The same set of equations is used for discharge cooling down (Equations 6 and 7).

$$\dot{Q}_{ex} = UA_{ex} \cdot \left( \frac{T_{ex1} \text{-} T_{ex}}{ln \dfrac{T_{ex} - T_w}{T_{ex1} - T_w}} \right) \tag{6}$$

$$\dot{Q}_{ex} = \dot{m} \cdot \left( h_{ex1} - h_{ex} \right) \tag{7}$$

Heat transfer towards the environment can be calculated using equation 8, where $T_{amb}$ is assumed to be constant and equal to 20 °C.

$$\dot{Q}_{amb} = UA_{amb} \cdot \left(T_w - T_{amb}\right)$$ (8)

During internal compression, the refrigerant state evolution follows equation 9 using a polytropic exponent n (equation 10). The nominal value of isentropic exponent γ is assumed to correspond to an evaporating temperature of 0 °C and a condensing temperature of 50 °C, taken as nominal operating conditions.

$$\dot{W}_{in} = \frac{n}{n-1} LP \cdot \dot{m} \cdot v_{su1} \cdot \left( \left( \frac{HP}{LP} \right)^{\frac{n-1}{n}} - 1 \right)$$ (9)

$$n = n_{nom} \frac{\gamma}{\gamma_{nom}}$$ (10)

Finally, the compressor shaft power is given by equation 11.

$$\dot{W} = \dot{W}_{in} + \dot{W}_{loss}$$ (11)

The other hypotheses made in this model are that pressure drops are neglected inside the compressor crankcase and heat transfer coefficients are constant.

### 3.5.2. Determination of parameters

In a first simulation, $UA_{su}$, $UA_{amb}$ and $UA_{ex}$ values are unknown. These coefficients are assumed to be constant parameters of the model. Their determination for R407C is carried out using experimental values of mass flow rate, input power and discharge temperature measured on our R407C prototype for nominal operating conditions. Table 3 shows the nominal values of main variables and parameters for an evaporating temperature of 0 °C and a condensing temperature of 50 °C at dew points. The nominal polytropic exponent $n_{nom}$ is assumed constant and equal to 1.4. The evaporation superheat of 5 K gives the value of $T_{su}$.

**Table 3:** Main variables and parameters at nominal conditions for R407C model

| Variable | $T_{ev}$ | $T_{cd}$ | $T_w$ | $T_{su}$ | $T_{su1}$ | $T_{ex1}$ | $T_{ex}$ | $\dot{m}$ | $\dot{W}$ | $UA_{su}$ | $UA_{amb}$ | $UA_{ex}$ |
|---|---|---|---|---|---|---|---|---|---|---|---|---|
| Unit | (°C) | (°C) | (°C) | (°C) | (°C) | (°C) | (°C) | (kg s$^{-1}$) | (W) | (W K$^{-1}$) | (W K$^{-1}$) | (W K$^{-1}$) |
| Value | 0.00 | 50.00 | 42.28 | 5.00 | 12.57 | 83.29 | 79.56 | 0.07217 | 4204 | 13.79 | 31.27 | 7.31 |

### 3.5.3. Model validation

The model validation is carried out using experimental results obtained on the R407C HPS prototype. The ranges of evaporating and condensing temperatures are respectively -7 °C to +10 °C and 40 °C to 55 °C. They correspond to the temperatures used in the applications of the HPS, which are domestic hot water preheating and space heating and cooling in oceanic climate regions. The following figures show satisfactory accordance between experimental and modelled values.

Figure 2 shows a correct agreement between experimental and modelled mass flow rates. The maximum discrepancy is less than 8.8 %. Dispersion of values can be explained by the quite low accuracy of experimental mass flow rate calculation. The heating capacity at the heat sink of the HPS was calculated using thermocouples and a water flow meter. The enthalpies of refrigerant were calculated using thermocouples and pressure sensors on the refrigeration circuit at the inlet and outlet of the condenser. The experimental mass flow rate was finally determined by dividing the heating capacity by the enthalpy difference. The errors were propagated by the calculations. In addition, transient phenomena were neglected during experimental measurements. Nevertheless, the accuracy of the model remains satisfactory at this stage of the study.

Figure 3 shows the comparison between experimental and modelled shaft power at the compressor. Lower values of input power are underestimated by the model down to -9.7 %. The maximal discrepancy is 8.8 %.

Figure 4 shows a correct agreement between experimental and modelled discharge temperature. Temperature differences are included in an interval from -5.2 K to +4.2 K. The discharge temperature will be used in the global heat pump model as an input variable for the condenser model. Therefore achieving satisfactory accuracy on this output variable is also very important.
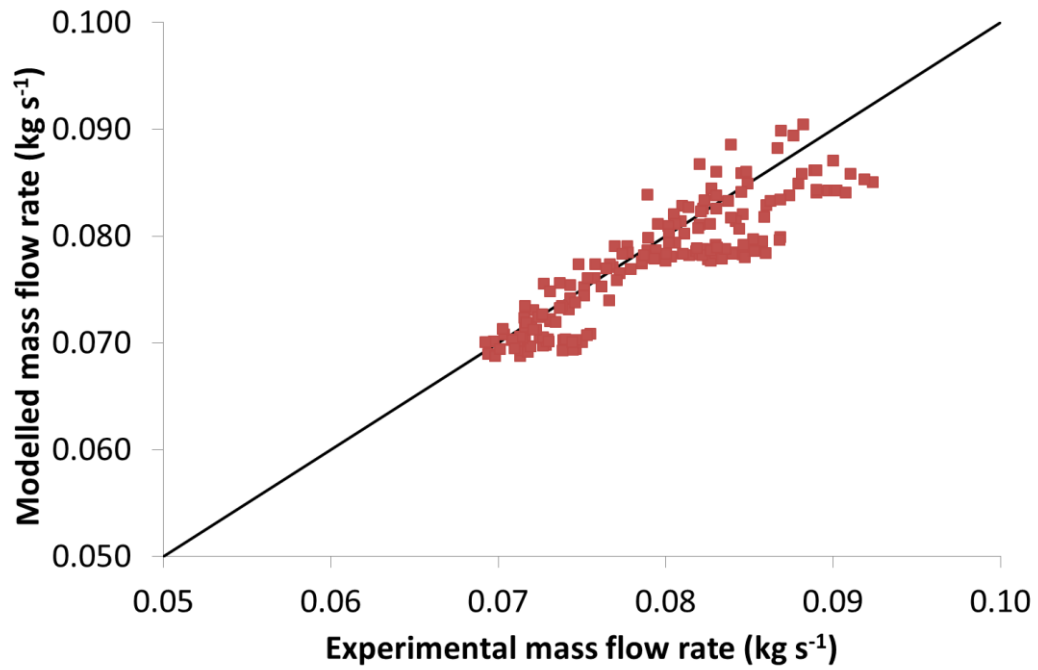
**Figure 2:** Comparison between experimental and modelled mass flow rate on R407C scroll compressor
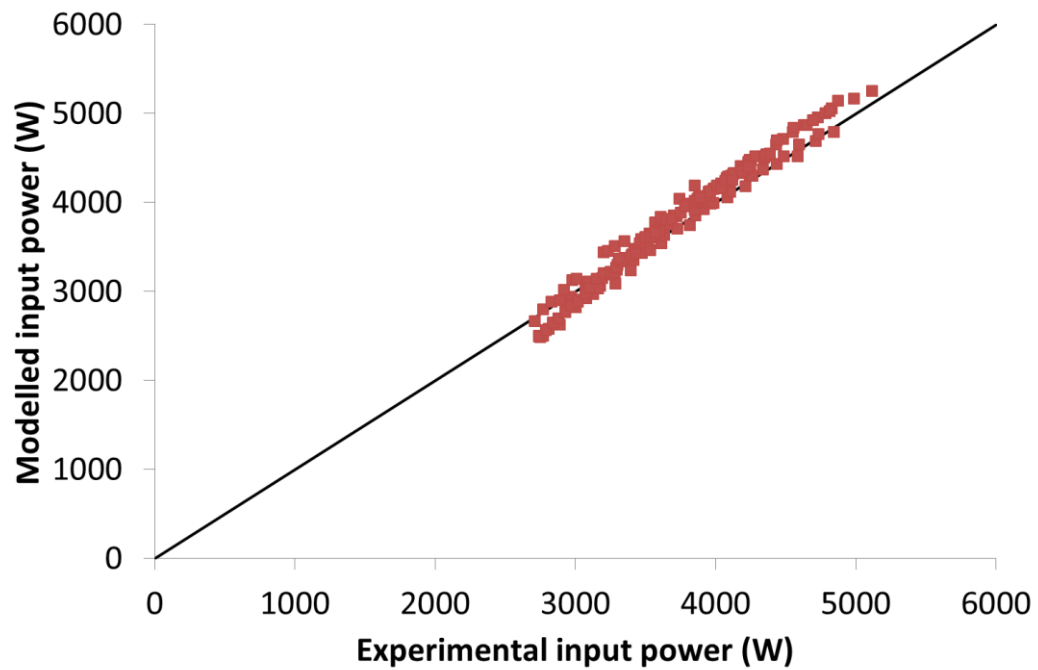


**Figure 3:** Comparison between experimental and modelled input power on R407C scroll compressor
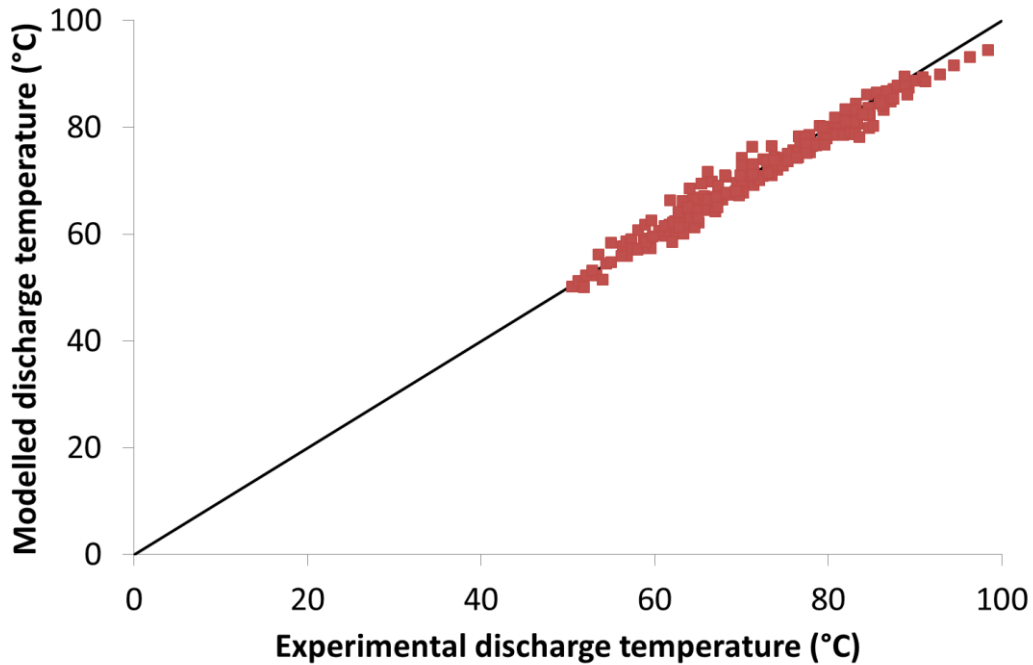
**Figure 4:** Comparison between experimental and modelled discharge temperature on R407C scroll compressor

## 4. SCROLL COMPRESSOR MODEL FOR HYDROCARBONS

### 4.1. Model adaptation to properties of hydrocarbons

New models correspond to the same compressor as in section 3.5 adapted to thermodynamic properties of hydrocarbons. In this section, the model adaptation is presented for hydrocarbons R290, R1270 and R600a.

### 4.1.1. Assumptions for model adaptation to hydrocarbons

The adaptation of the model was inspired by Duprez et al. (2010) and consists in recalculating the heat transfer coefficients at suction $UA_{su}$ and discharge $UA_{ex}$ for nominal conditions of evaporation at 0 °C and condensation of 50 °C. UA values are assumed constant for other operating conditions. The U value is assumed to be calculated using the Nusselt number following equation 12. The Nusselt number Nu and the conductivity $\lambda$ depend on the fluid. The Nusselt number is given by Dittus-Boelter correlation (equation 13), where parameter m is equal to 0.4 for the suction heating process and 0.3 for the discharge cooling process. The Reynolds number Re depends on the viscosity $\nu$ of the fluid (equation 14). In equations 12 to 14, velocity u (linked to swept volume $V_s$) and hydraulic diameter D are geometric parameters of the scroll

compressor and are the same for hydrocarbons as for R407C. The refrigerant velocity in suction and exhaust sections is kept constant for the two different fluids because velocity is assumed to be driven by the moving scroll of the compressor and density is assumed constant during these pre- and post-transformations of the refrigerant. Therefore the adaptation to hydrocarbons properties results in equation 15 for $UA_{su}$ and $UA_{ex}$ values. $UA_{amb}$ corresponds to the heat transfer between the crankcase and the ambiance. This parameter is independent on the refrigerant and has the same value as for R407C.

$$U = \frac{Nu \cdot \lambda}{D} \tag{12}$$

$$Nu = 0.023 \cdot Re^{0.8} \cdot Pr^{m} \tag{13}$$

$$Re = \frac{u \cdot D}{\nu} \tag{14}$$

$$UA_{HC} = UA_{R407C} \cdot \left(\frac{\nu_{R407C}}{\nu_{HC}}\right)^{0.8} \cdot \left(\frac{Pr_{HC}}{Pr_{R407C}}\right)^{m} \cdot \left(\frac{\lambda_{HC}}{\lambda_{R407C}}\right) \tag{15}$$

A second adaptation is carried out on the polytropic exponent $n_{HC}$ used in equation 9. It is recalculated depending on the ratio of isentropic exponents $\gamma_{HC}$ and $\gamma_{R407C}$ (equation 16). The nominal values are taken for R407C.

$$n_{HC} = n_{R407C} \cdot \left(\frac{\gamma_{HC}}{\gamma_{R407C}}\right) \tag{16}$$

The adaptation process results to take into account nominal thermodynamic properties of R407C and hydrocarbons reported in table 4. Prandtl numbers and conductivities show similar values. The viscosities of hydrocarbons are higher than the viscosity of R407C. Nominal thermodynamic properties give nominal UA values reported in table 5. R600a shows lower UA values because of higher viscosity. R290 and R1270 have nominal viscosity values between R407C and R600a and higher conductivity values that result in a compensation to reach similar heat transfer coefficients to those of R407C.

**Table 4:** Values of thermodynamic properties at nominal conditions for R407C and HC models

| Refrigerant | $Pr_{su}$ (-) | $\lambda_{su}$ (W m$^{-1}$ K$^{-1}$) | $\nu_{su}$ (m$^2$ s$^{-1}$) | $Pr_{ex}$ (-) | $\lambda_{ex}$ (W m$^{-1}$ K$^{-1}$) | $\nu_{ex}$ (m$^2$ s$^{-1}$) | $\gamma$ (-) | $n$ (-) |
|---|---|---|---|---|---|---|---|---|
| R407C | 0.776 | 0.0137 | $7.263\cdot10^{-7}$ | 0.883 | 0.0184 | $1.955\cdot10^{-7}$ | 1.187 | 1.400 |
| R290 | 0.827 | 0.0180 | $8.898\cdot10^{-7}$ | 1.045 | 0.0236 | $2.663\cdot10^{-7}$ | 1.198 | 1.412 |
| R1270 | 0.863 | 0.0169 | $7.923\cdot10^{-7}$ | 1.057 | 0.0228 | $2.463\cdot10^{-7}$ | 1.237 | 1.458 |
| R600a | 0.839 | 0.0157 | $1.939\cdot10^{-6}$ | 0.916 | 0.0197 | $4.993\cdot10^{-7}$ | 1.124 | 1.326 |

**Table 5:** UA values at nominal conditions for R407C and HC models

| Refrigerant | $UA_{su}$ (W K$^{-1}$) | $UA_{ex}$ (W K$^{-1}$) |
|---|---|---|
| R407C | 13.79 | 7.31 |
| R290 | 15.85 | 7.69 |
| R1270 | 16.60 | 7.93 |
| R600a | 7.46 | 3.72 |

### 4.1.2. Comparison of R407C and HC compressors

A numerical comparison of mass flow rates, input powers and discharge temperatures is carried out between R407C and hydrocarbons in the same range of evaporating temperatures (-10 °C to +10 °C) and condensing temperatures (40 °C to 60 °C).

Figure 5 shows the mass flow rate of hydrocarbons compared to the one of R407C using the same compressor. The ratio between R407C and hydrocarbons values is nearly constant. The R290 mass flow rate is 45.4 % lower than the R407C one in average. The hydrocarbon compressor size cannot be reduced compared to R407C ones because the density of hydrocarbons is lower by almost the same proportion. Moreover, this discrepancy could act in an unfavourable manner for R290 scroll compressor because the heating or cooling capacities are proportional to the mass flow rate. Nevertheless the ratio of latent heat recoverable by condensation at 50 °C of R407C over the one of R290 is in the same proportion than the inverse ratio of mass flow rates. So the heating capacity recoverable by implementing R290 instead of R407C should be somewhat equivalent. The same interpretation can be carried out with R1270. However, R600a shows a much lower mass flow rate that cannot be compensated by a higher enthalpy difference at condensation.

Figure 6 presents the comparison between input powers. The average variations for refrigerants R290, R1270 and R600a are -12.5 %, +6.8 % and -63.9 %. R600a again shows much lower values. Taking into account the low mass flow rate and the low input power, equivalent COPs such as presented in table 1 can be achieved with R600a.

Figure 7 shows the difference between discharge temperatures using R407C and hydrocarbon models. The difference varies from 6.5 K to 19.0 K for propane, from 2.3 K to 8.9 K for propylene and from 13.2 K to 34.1 K for isobutane. This factor increases the longevity of the compressor and reduces oil ageing. Besides, the heat recovered during desuperheating will decrease compared to an operation with the same discharge temperatures as the ones of R407C. However, the specific heat of hydrocarbons is around twice the one of R407C in vapour phase at these pressures. So the heating capacity recoverable during the desuperheating process using hydrocarbons will be equivalent or even higher than that of R407C.
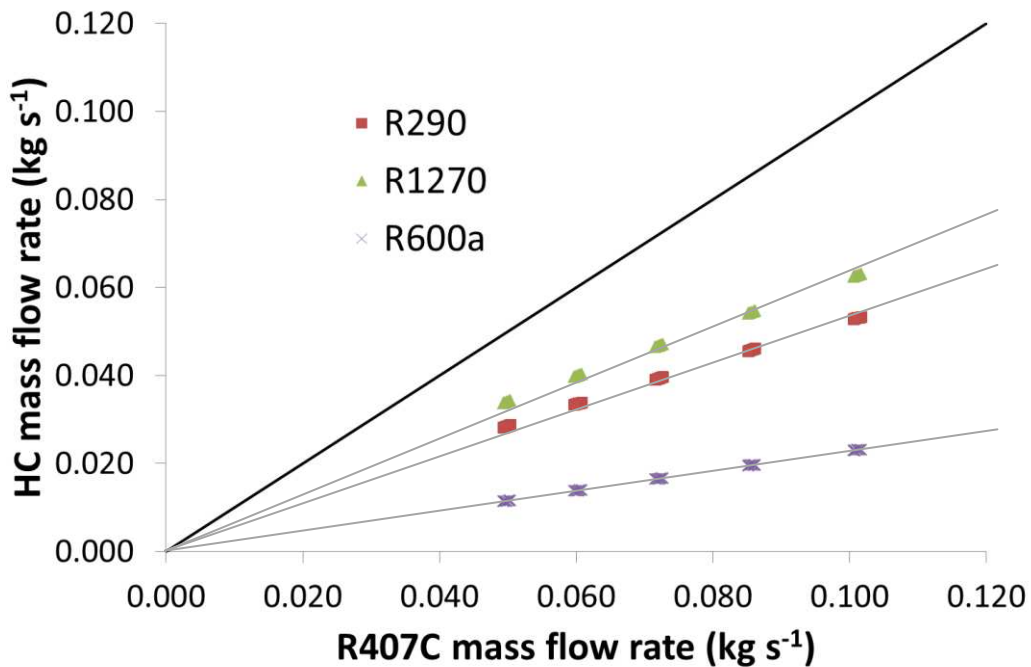


**Figure 5:** Comparison between R407C and HC modelled mass flow rates
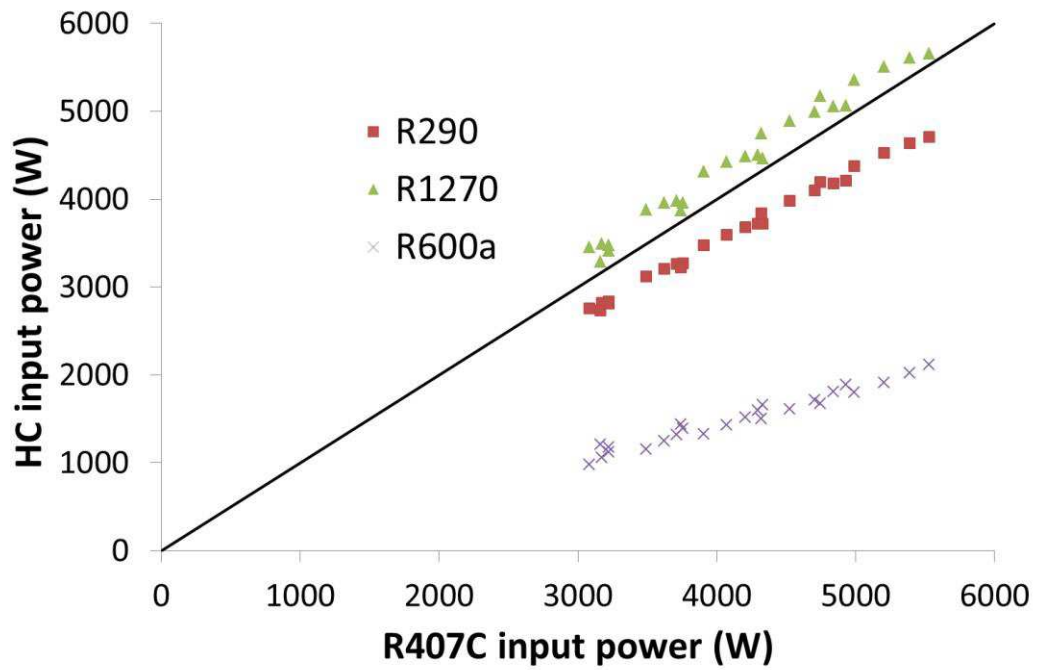
**Figure 6:** Comparison between R407C and HC modelled input powers
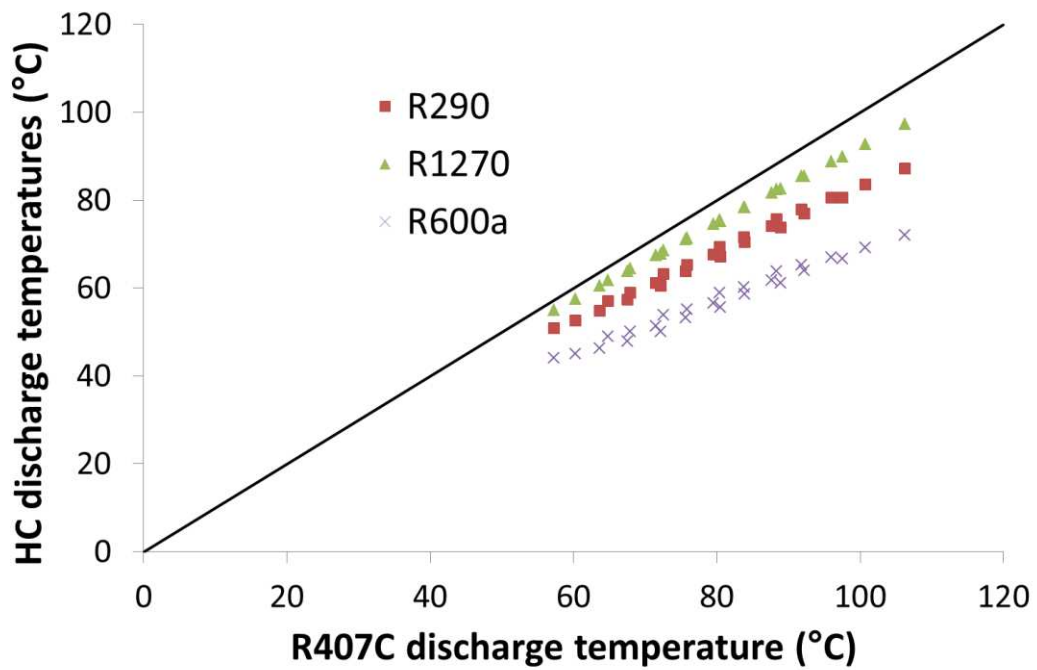


**Figure 7:** Comparison between R407C and HC modelled discharge temperatures

23

### 4.2. Model adaptation to other sizes of compressor

#### 4.2.1. Equation for model adaptation to other sizes of compressor

The adaptation to another size of compressor influences the UA values of the model. The heat transfer coefficient U is assumed constant. The evolution of heat transfer area follows the dimensional analysis concept. The following assumptions are made regarding the geometry of the compressor:

- The compressor is a cube with an edge of length e.

- The volume of the cube $e^3$ is proportional to the swept volume.

- Heat transfer areas used in UA values are proportional to the surface area of the cube $6e^2$ submitted to heat exchange.

The new heat transfer area A is assumed to be calculated using the original heat transfer area $A_0$ and the ratio of new and original swept volumes following equation 17.

$$\frac{A}{A_0} = \left(\frac{V_s}{V_{s0}}\right)^{\frac{2}{3}}$$

(17)

#### 4.2.2. Comparison with experimental results

Two HFC compressors were tested with two hydrocarbons by a compressor manufacturer (Arnemann, 2012). The first compressor has a swept volume of 6.8 $m^3$ $h^{-1}$ and was tested with propane. The second compressor has a swept volume of 19.8 $m^3$ $h^{-1}$ and was tested with propylene. Figure 8 shows the comparison of input powers with modelled values. The evaporating temperature is -10 °C. The condensing temperature varies from 30 to 60 °C. The ratios of modelled input powers over experimental values are close to 1. The minimum and maximum discrepancies are equal to -6.5 % and +4.1 %. Therefore the model validation is considered as extended to propylene for the operating conditions considered. The adaptation to other sizes of compressor works for either a size increase or decrease.
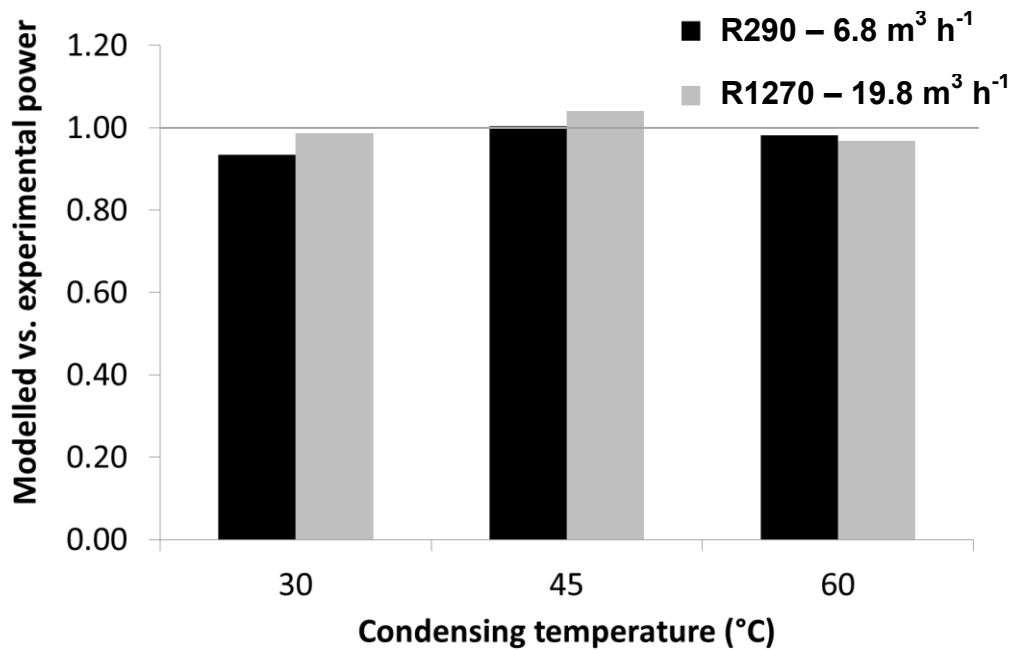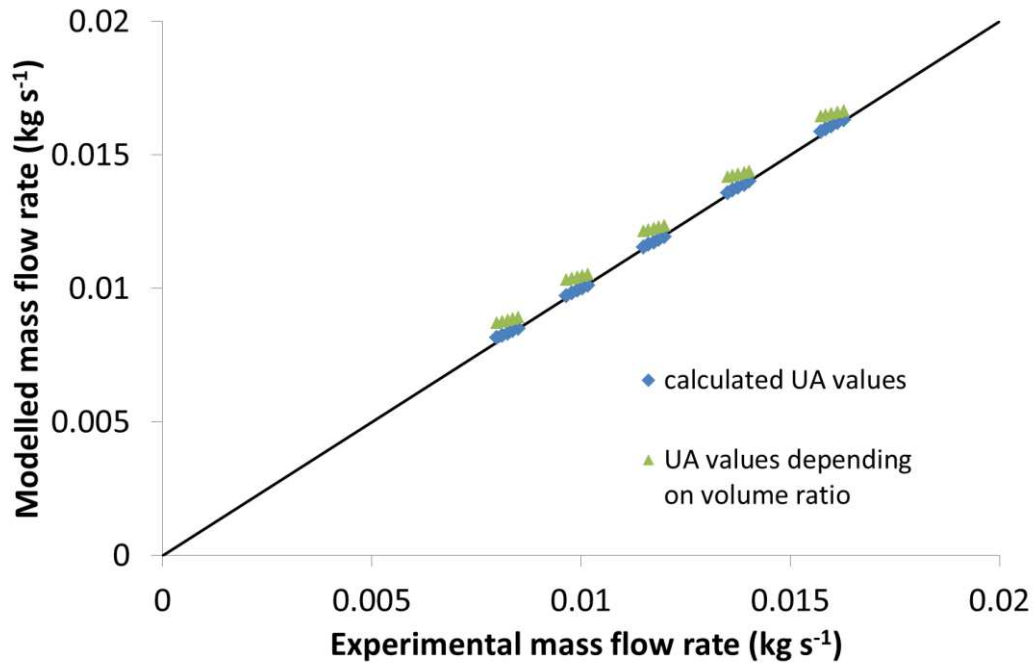
**Figure 8:** Comparison of modeled input power to experimental data of compressor manufacturer.

The compressor manufacturer also provided a larger set of experimental data on a 4.68 m$^3$ h$^{-1}$ swept volume compressor. The same adaptation procedure was applied to calculate the mass flow rate, the input power and the discharge temperature. The results correspond to the values shown in triangles (UA values depending on volume ratio) on figures 9 to 11. The adaptation procedure does not work for this compressor because of errors made on the calculation of UA values. The minimum and maximum discrepancies are 2.33 % and 8.95 % on mass flow rate, -0.81 % and 20.61 % on input power and the discharge temperature difference is between -9.82 K and -3.82 K. An acceptable validation of the model was obtained using the same procedure as for the validation of the R407C compressor model in section 4 of the article. The values $UA_{su}$, $UA_{ex}$ and $UA_{amb}$ were recalculated using the experimental values of mass flow rate, input power and discharge temperature for one operating point at nominal conditions ($T_{ev} = 0$ °C and $T_{cd} = 50$ °C). The results with calculated UA values are represented in diamonds on figures 9 to 11. The discrepancies are -0.50 % and +2.05 % on mass flow rate, -15.30 % and 3.09 % on input power and the discharge temperature difference is between -4.35 K and +0.98 K. The lowest discrepancy on input power appears for operating conditions corresponding to very low heating or cooling demand ($T_{ev} = 10$ °C and $T_{cd} = 40$ °C). The second lowest discrepancy on input power is -10.06 %. The UA values for the two models (UA values depending on volume ratio and calculated UA values) are shown in table 6. The heat transfers at the suction heating-up of

the refrigerant and between the crankcase of the compressor and the ambiance were respectively underestimated and overestimated. The difference can be explained by the insulation of the compressor implemented during the test campaign that was carried out by the compressor manufacturer. The insulation reduces the $UA_{amb}$ value by adding a high thermal resistance in the U calculation. It also produces a higher temperature on the surface of the crankcase. The effective wall temperature $T_w$ is higher than the modelled one supposed to be the average between suction and exhaust temperatures (equation 2). To compensate this phenomenon, $UA_{su}$ value increases. $UA_{ex}$ values are in the same order of magnitude.

**Table 6:** UA values at nominal conditions for compressor models with calculated UA values and UA values depending on volume ratio
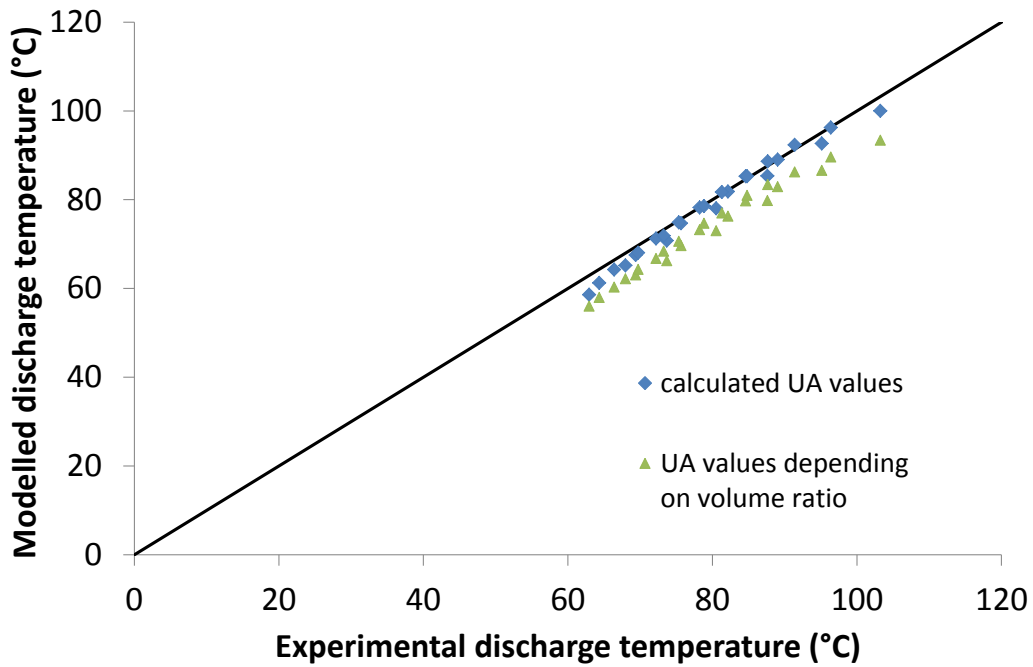
| UA values | $UA_{su}$ (W K$^{-1}$) | $UA_{ex}$ (W K$^{-1}$) | $UA_{amb}$ (W K$^{-1}$) |
|---|---|---|---|
| From size adaptation | 6.49 | 3.58 | 14.71 |
| Calculated UA values | 16.74 | 5.75 | 2.05 |



**Figure 9:** Comparison of modelled and experimental mass flow rate of the 4.68 m$^3$ h$^{-1}$ compressor.
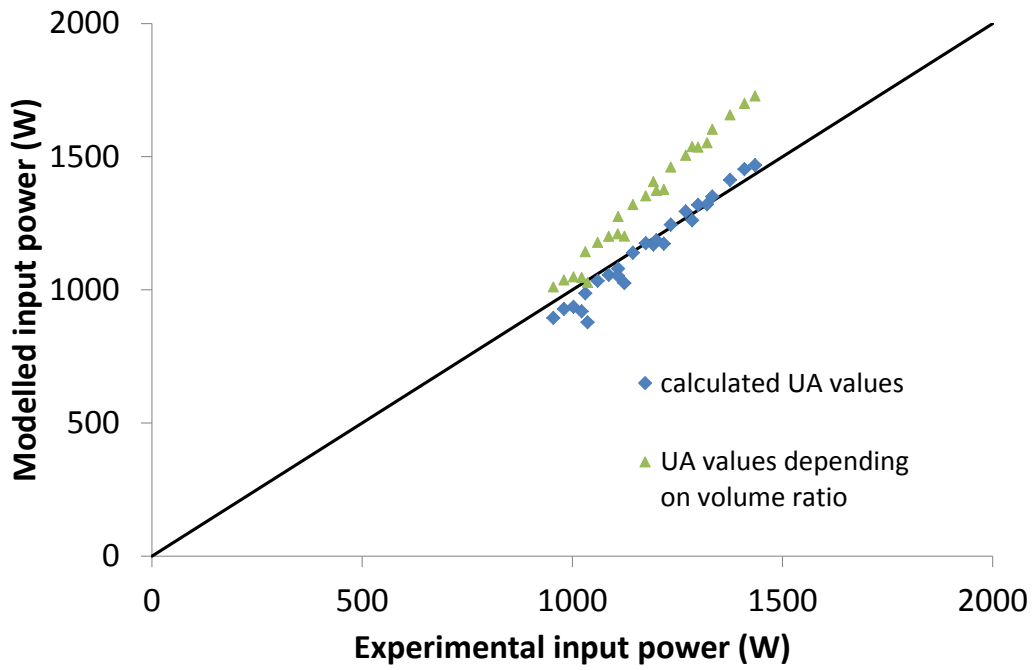
**Figure 10:** Comparison of modelled and experimental input power of the 4.68 m$^3$ h$^{-1}$ compressor.



**Figure 11:** Comparison of modelled and experimental discharge temperature of the 4.68 m$^3$ h$^{-1}$ compressor.

# 5. CONCLUSIONS AND PERSPECTIVES

A thermodynamically realistic R407C scroll compressor model was developed and adapted to hydrocarbons, which are promising fluids regarding the evolution of international regulations on environmental impact of refrigerants. A dimensional analysis was performed to adapt the model to other compressor sizes. The semi-empirical Winandy et al. (2002a) model was used with some assumptions made by Duprez et al. (2007 and 2010). The wall temperature was assumed to be constant and equal to the average between suction and discharge temperatures. The main difference concerns the internal power calculation using a polytropic evolution during compression. The model considers constant heat transfer coefficients at suction heating-up, discharge cooling down and transfer to the ambient. Only one nominal operating point is necessary to set these parameters. The scroll compressor modelling, the adaptation procedures to other fluids and to other sizes were validated for R407C and propane in terms of mass flow rate, compressor power and discharge temperature with accuracies less than respectively ±10 %, ±10 % and ±5 K in typical operating conditions. The validation was extended to propylene in terms of compressor power. The scroll compressor model validation still needs to be extended to other fluids and other size changes with other experimental data. During the model development, we noticed that there is a non-negligible sensitivity of UA values depending on the refrigerant type, the wall temperature and the presence of insulation on the compressor crankcase. The comparison study between R407C and hydrocarbon models concludes a possible performance improvement by implementing R290, R1270 or R600a in the R407C scroll compressor. This hydrocarbon scroll compressor model can be utilized in more global heat pump models for seasonal performance evaluation. Some improvements can be made, namely on the oil temperature and the location of the suction pipe that could also have an influence. For some compressors, the suction port can be situated at the bottom and for others not. Therefore the refrigerant flow passes or not through the motor before reaching the suction scroll pocket. These features could be taken into account if more accuracy is requested.

This study is part of a research project on heat pumps for simultaneous heating and cooling. A near-industrial propane prototype with a semi-hermetic piston-type compressor was built. Even if a propane detection device was installed, a document was signed to release the compressor manufacturer of any responsibility in case of accident. No manufacturer would have sold us a scroll compressor for

hydrocarbons. No apparent regulation is more stringent for scroll than for reciprocating compressors but the feebleness must be due to the youth of the technology and the lack of knowledge on long term reliability of scroll compressors. The flammability issue of hydrocarbons is still the main concern in the field of low to medium capacity heat pumps and if the technology were proved to be safe, important changes in regulations still have to be made to envisage a widespread of hydrocarbon heat pumps.

## ACKNOWLEDGEMENTS

## REFERENCES

Adamson, B.M., 2008. Application of hydrocarbon refrigerants with scroll compressors in low temperature cascade systems. In: Proceedings of the IIR Gustav Lorentzen Conference on Natural Refrigerants, Copenhagen, Denmark, IIF/IIR, 126-130.

Arnemann, H., Bella, B., Kaemmer ,N., Nohales, J., 2012. Scroll compressor assessment with R-290 and R-1270. In: Proceedings of the 10th IIR Gustav Lorentzen Conference on Natural Refrigerants, Delft, the Netherlands, IIF/IIR, paper No GL-308.

Blunier, B., Cirrincione, G., Herve, Y., Miraouia, A., 2009. A new analytical and dynamical model of a scroll compressor with experimental validation. International Journal of Refrigeration 32, 874-891.

Byrne, P., Miriel, J., Lénat, Y., 2009. Design and simulation of a heat pump for simultaneous heating and cooling using HFC or $CO_2$ as a working fluid. International Journal of Refrigeration 32, 1711-1723.

Byrne, P., Miriel, J., Lénat, Y., 2011a. Experimental study of an air-source heat pump for simultaneous heating and cooling – part 1: basic concepts and performance verification. Applied Energy 88, 1841-1847.

Byrne, P., Miriel, J., Lénat, Y., 2011b. Experimental study of an air-source heat pump for simultaneous heating and cooling – part 2: dynamic behaviour and two-phase thermosiphon defrosting technique. Applied Energy 88, 3072-3078.

Byrne, P., Miriel, J., Lénat, Y., 2012. Modelling and simulation of a heat pump for simultaneous heating and cooling. Building Simulation: An International Journal 5, 219–232.

Byrne, P., 2013. Advances in air-source heat pump water heaters. In: Novel Concepts for Energy-Efficient Water Heating Systems: Theoretical Analysis and Experimental Investigation. Commercial editor: Nova Science Publishers, Inc. Scientific editors: Barbin D. F., Silveira Jr. V. Chapter 4, 93-122.

Chen, Y., Halm, N.P., Groll, E.A., Braun, J.E., 2002a. Mathematical modeling of scroll compressors - part I: compression process modelling. International Journal of Refrigeration 25, 731-750.

Chen, Y., Halm, N.P., Braun, J.E., Groll, E.A., 2002b. Mathematical modeling of scroll compressors - part II: overall scroll compressor modeling. International Journal of Refrigeration 25, 751-764.

Choi, J.W., Lee, G., Kim, M.S., 2011. Numerical study on the steady state and transient performance of a multi-type heat pump system. International Journal of Refrigeration 34, 429-443.

Cuevas, C., Lebrun, J., 2009. Testing and modelling of a variable speed scroll compressor. Applied Thermal Engineering 29, 469-478.

Cuevas, C., Lebrun, J., Lemort, V., Winandy, E., 2010. Characterization of a scroll compressor under extended operating conditions. Applied Thermal Engineering 30, 605–615.

Cuevas, C., Fonseca, N., Lemort, V., 2012. Automotive electric scroll compressor: Testing and modeling. International Journal of Refrigeration 35, 841-849.

Duprez, M.E., Dumont, E., Frère, M., 2007. Modelling of reciprocating and scroll compressors. International Journal of Refrigeration 30, 873-886.

Duprez, M.E., Dumont, E., Frère, M., 2010. Modeling of scroll compressors – Improvements. International Journal of Refrigeration 33, 721-728.

European Standard EN 378, 2008. Refrigerating systems and heat pumps – Safety and environmental requirements.

European Standard EN 60079-10-1, 2009. Explosive atmospheres. Classification of areas.

European Standard EN14511-3, 2004. Air conditioners, liquid chilling packages and heat pumps with electrically driven compressors for space heating and cooling -Part 3: Test methods.

Granryd, E., 2001. Hydrocarbons as refrigerants – an overview. International Journal of Refrigeration 24, 15-24.

Guo, J.J., Wu, J.Y., Wang, R.Z., Li, S., 2011. Experimental research and operation optimization of an air-source heat pump water heater. Applied Energy 88, 4128-4138.

Halimic, E., Ross, D., Agnew, B. Anderson, A., Potts, I., 2003. A comparison of the operating performance of alternative refrigerants. Applied Thermal Engineering 23, 1441–1451.

Jiang, Z., Harrison, D.K., Cheng, K., 2003. Computer-aided design and manufacturing of scroll compressors. Journal of Materials Processing Technology 138, 145–151.

Kim, J.H., Ahn, J.M., Cho, S.O., Cho, K.R., 2008. Numerical simulation on scroll expander–compressor unit for $CO_2$ trans-critical cycles. Applied Thermal Engineering 28, 1654-1661.

Kinab, E., Marchio, D., Rivière P., Zoughaib, A., 2010. Reversible heat pump model for seasonal performance optimization. Energy and Buildings 42, 2269-2280.

Klein, S.A., Alvarado, F.L., 1992. EES – Engineering Equation Solver, F-Chart software, Wisconsin, USA.

Lee, C.K., Lam, H.N., 2013. A comparison of different generalised modelling approaches for a scroll refrigerant compressor, International Journal of Refrigeration (2013), doi: 10.1016/j.ijrefrig.2013.01.002

Li, W., 2012. Simplified steady-state modeling for hermetic compressors with focus on extrapolation. International Journal of Refrigeration 35, 1722-1733.

Li, W., 2013. Simplified steady-state modeling for variable speed compressor. Applied thermal engineering 50, 318-326.

Liu, Y., Hung, C., Chang, Y., 2009. Mathematical model of bypass behaviors used in scroll compressor. Applied Thermal Engineering 29, 1058-1066.

Liu, Y., Hung, C., Chang, Y., 2010. Design optimization of scroll compressor applied for frictional. International Journal of Refrigeration 33, 615-624.

Madani, H., Claesson, J., Lundqvist, P., 2011. Capacity control in ground source heat pump systems. Part I: modeling and simulation. International Journal of Refrigeration 34, 1338-1347.

Navarro, E., Corberan, J.M., Martinez-Galvan, I.O., Gonzalvez, J., 2012. Oil sump temperature in hermetic compressors for heat pump applications. International Journal of Refrigeration 35, 397-406.

Ooi, K.T., Zhu, J., 2004. Convective heat transfer in a scroll compressor chamber a 2-D simulation. International Journal of Thermal Sciences 43, 677-688.

Palm, B., 2008. Hydrocarbons as refrigerants in small heat pump and refrigeration systems – A review. International Journal of Refrigeration 31, 552–563.

Park, Y.C., Kim, Y., Cho, H., 2002. Thermodynamic analysis on the performance of a variable speed scroll compressor with refrigerant injection. International Journal of Refrigeration 25, 1072-1082.

Qiang, J., Peng, B., Liu, Z., 2013a. Dynamic model for the orbiting scroll based on the pressures in scroll chambers–Part I: Analytical modeling, International Journal of Refrigeration (2013), doi: 10.1016/j.ijrefrig.2013.02.004.

Qiang, J., Peng, B., Liu, Z., 2013b. Dynamic model for the orbiting scroll based on the pressures in scroll chambers–Part II: Investigations on scroll compressors and model validation, International Journal of Refrigeration (2013), doi: 10.1016/j.ijrefrig.2013.02.013

Rong, C., Wen, A., 2009. Discussion on leaking characters in meso-scroll compressor. International Journal of Refrigeration 32, 1433-1441.

Sun, S., Zhao, Y., Li, L., Shu, P., 2010. Simulation research on scroll refrigeration compressor with external cooling. International Journal of Refrigeration 33, 897-906.

Techarungpaisan, P., Theerakulpisut, S. Priprem, S., 2007. Modeling of a split type air conditioner with integrated water heater. Energy Conversion and Management 48, 1222-1237.

Technical University of Denmark, 1998. Department of Mechanical Engineering. Coolpack, a collection of simulation tools for refrigeration. Version 1.46.

Tseng, C.H., Chang, Y.C., 2006. Family design of scroll compressors with optimization. Applied Thermal Engineering 26, 1074-1086.

Wang, B., Li, X., Shi, W., 2005. A general geometrical model of scroll compressors based on discretional initial angles of involute. International Journal of Refrigeration 28, 958-966.

Wang, B., Shi, W., Li, X., Yan, Q., 2008. Numerical research on the scroll compressor with refrigeration injection. Applied Thermal Engineering 28, 440-449.

Winandy, E., Saavedra, C., Lebrun, J., 2002a. Experimental analysis and simplified modelling of a hermetic scroll refrigeration compressor. Applied Thermal Engineering 22, 107-120.

Winandy, E., Lebrun, J., 2002b. Scroll compressors using gas and liquid injection: experimental analysis and modelling. Int. J. Refrigeration 25, 1143-1156.